

# The White Paper on ELLAM Implementation in C++

Jiangguo (James) Liu <sup>1</sup>

March 11, 2009

<sup>1</sup>Department of Mathematics, Colorado State University, Fort Collins, CO  
80523-1874, USA, [liu@math.colostate.edu](mailto:liu@math.colostate.edu)



# Contents

<b>1</b>	<b>ELLAM for IBVP of Convection-Diffusion Equations</b>	<b>9</b>
1.1	Problem . . . . .	9
1.2	Time Discretization and Localized Test Functions . . . . .	10
1.3	Characteristics . . . . .	11
1.4	Adjoint Equation . . . . .	12
1.5	Boundaries, Flows, and Tracking . . . . .	13
1.6	Approximations of Diffusion and Source Terms . . . . .	14
1.7	Decomposition of Boundary Term . . . . .	15
1.8	Reference Equation . . . . .	16
<b>2</b>	<b>Finite Element Methods within ELLAM Framework</b>	<b>17</b>
2.1	Partitions of Spatial Domain and Outflow Space-Time Boundary and Courant Number . . . . .	17
2.2	Two Groups of Trial and Test Functions . . . . .	18
2.3	Interior Nodes and Noflow Boundary . . . . .	19
2.4	Inflow Boundary Conditions . . . . .	19
2.5	Outflow Boundary Conditions . . . . .	20
2.6	FEM Assembly . . . . .	21
<b>3</b>	<b>Implementation</b>	<b>23</b>
3.1	Assumptions on Problem and Method . . . . .	23
3.2	FEM Assembly . . . . .	24
3.3	Mesh and Timing . . . . .	25
3.4	Numerical Integration . . . . .	25
3.5	Matrices for the Reference Element . . . . .	26
3.5.1	Mass Matrix for the Reference Element . . . . .	27
3.5.2	Stiffness Matrix for the Reference Element . . . . .	27
3.5.3	Source RHS for the Reference Element . . . . .	28

3.6	Matrices on General Elements . . . . .	29
3.6.1	Mass Matrix . . . . .	29
3.6.2	Stiffness Matrix . . . . .	29
3.6.3	Source RHS . . . . .	30
3.7	Assembly of Element Matrices and RHS . . . . .	31
3.8	Linear Solvers . . . . .	32
3.9	Characteristic Tracking . . . . .	33
3.10	Examples . . . . .	34
<b>4</b>	<b>Source Code of a Mini Version ELLAM</b>	<b>37</b>
4.1	MiniELLAM: Head File . . . . .	37
4.2	MiniELLAM: Source Code . . . . .	38
4.3	Mini ELLAM: Examples . . . . .	57
<b>A</b>	<b>List of Abbreviations</b>	<b>63</b>

# List of Tables

3.1	Frequently used standard quadratures . . . . .	26
3.2	A typical rectangular element and its neighboring nodes . . .	31



# List of Figures

1.1	<i>Flows, characteristics, and boundaries . . . . .</i>	14
3.1	A typical rectangular element and its neighboring nodes . . .	31



# Chapter 1

## ELLAM for IBVP of Convection-Diffusion Equations

### 1.1 Problem

Let  $\Omega$  be a (not necessarily rectangular) domain in  $\mathbb{R}^d$  ( $d = 1, 2,$  or  $3$ ) and  $[0, T]$  be a time period. We consider the following linear convection-diffusion equation:

$$(1.1) \quad (Ku)_t + \nabla \cdot (\mathbf{V}u - \mathbf{D}\nabla u) + Ru = f(\mathbf{x}, t), \quad \mathbf{x} \in \Omega, \quad t \in (0, T],$$

where where

$K(\mathbf{x}, t)$	retardation
$\mathbf{V}(\mathbf{x}, t)$	velocity
$\mathbf{D}(\mathbf{x}, t)$	diffusion
$R(\mathbf{x}, t)$	reaction
$f(\mathbf{x}, t)$	source/sink

$u(\mathbf{x}, t)$  is the unknown function,  $K(\mathbf{x}, t)$  is a retardation coefficient,  $\mathbf{V}(\mathbf{x}, t)$  is a fluid velocity field,  $\mathbf{D}(\mathbf{x}, t)$  is a diffusion-dispersion tensor, and  $f(\mathbf{x}, t)$  is a source term. It is assumed that  $K(\mathbf{x}, t)$  has positive lower and upper bounds. In addition,  $\mathbf{D}(\mathbf{x}, t)$  is taken as a real symmetric positive definite matrix with uniform lower and upper bounds for its eigenvalues that are independent of  $(\mathbf{x}, t)$ .

An initial condition

$$(1.2) \quad u(\mathbf{x}, 0) = u_0(\mathbf{x}), \quad \mathbf{x} \in \Omega$$

is posed as usual. But boundary conditions needs more attention.

Let  $\partial\Omega$  be the boundary of  $\Omega$ , then we can decompose the space-time boundary  $\Gamma := \partial\Omega \times [0, T]$  as  $\Gamma = \Gamma^I \cup \Gamma^O \cup \Gamma^N$  where

$$(1.3) \quad \begin{aligned} \Gamma^I &:= \{(\mathbf{x}, t) \mid \mathbf{x} \in \partial\Omega, t \in [0, T], \mathbf{V}(\mathbf{x}, t) \cdot \mathbf{n}(\mathbf{x}) < 0\} \\ \Gamma^O &:= \{(\mathbf{x}, t) \mid \mathbf{x} \in \partial\Omega, t \in [0, T], \mathbf{V}(\mathbf{x}, t) \cdot \mathbf{n}(\mathbf{x}) > 0\} \\ \Gamma^N &:= \{(\mathbf{x}, t) \mid \mathbf{x} \in \partial\Omega, t \in [0, T], \mathbf{V}(\mathbf{x}, t) \cdot \mathbf{n}(\mathbf{x}) = 0\} \end{aligned}$$

are the inflow, outflow, and noflow boundaries, respectively, and  $\mathbf{n}(\mathbf{x})$  is the outward unit normal vector.

In general, an inflow boundary during one time period might become an outflow or a noflow boundary in the next time period or vice versa.

On the noflow boundary, we have

$$(1.4) \quad (\mathbf{V}u - \mathbf{D}\nabla u) \cdot \mathbf{n} \equiv 0.$$

On the inflow or outflow boundary, one can mathematically specify Dirichlet, Neumann, or Robin ( total flux ) condition:

$$(1.5) \quad \begin{aligned} u(\mathbf{x}, t) &= g_1^{type}(\mathbf{x}, t), & (\mathbf{x}, t) \in \Gamma^{type}, & \text{Dirichlet} \\ -\mathbf{D}\nabla u(\mathbf{x}, t) \cdot \mathbf{n} &= g_2^{type}(\mathbf{x}, t), & (\mathbf{x}, t) \in \Gamma^{type}, & \text{Neumann} \\ (\mathbf{V}u - \mathbf{D}\nabla u)(\mathbf{x}, t) \cdot \mathbf{n} &= g_3^{type}(\mathbf{x}, t), & (\mathbf{x}, t) \in \Gamma^{type}, & \text{Robin} \end{aligned}$$

where  $type = I$  or  $O$  represents the inflow or outflow boundary type. In applications, however, an inflow Dirichlet or Robin condition and an outflow Dirichlet or Neumann condition are often posed. For example, common boundary conditions in petroleum reservoir simulation are noflow boundary conditions. For groundwater contamination simulation, a Dirichlet or Robin condition is usually specified at the inflow boundary while a Dirichlet or Neumann boundary condition is posed at the outflow boundary.

## 1.2 Time Discretization and Localized Test Functions

Let  $0 = t_0 < t_1 < \dots < t_{n-1} < t_n < \dots < t_N = T$  be a partition of  $[0, T]$  with  $\Delta t_n := t_n - t_{n-1}$ .

We choose test functions  $w(\mathbf{x}, t) \in H^1(\Omega \times [0, T])$  in such a way that they vanish outside the space-time strip  $\Omega \times (t_{n-1}, t_n]$  and are discontinuous in time at time  $t_{n-1}$ . Then integration (in time) by parts, or to be accurate, Green's formula, leads us to the following weak formulation:

Find  $u(\mathbf{x}, t) \in H^1(\Omega \times (0, T])$  so that for any test function  $w(\mathbf{x}, t)$ , the following equation holds

$$(1.6) \quad \begin{aligned} & \int_{\Omega} (Ru w)(\mathbf{x}, t_n) d\mathbf{x} + \int_{J_n} \int_{\Omega} (\mathbf{D}\nabla u) \cdot \nabla w \, dx dt \\ & + \int_{\Gamma_n} (\mathbf{V}u - \mathbf{D}\nabla u) \cdot \mathbf{n} w \, dy dt - \int_{\Sigma_n} u(w_t + \mathbf{V} \cdot \nabla w) \, dx dt \\ & \int_{\Omega} (Ru w)(\mathbf{x}, t_{n-1}^+) d\mathbf{x} + \int_{\Sigma_n} f(\mathbf{x}, t) w(\mathbf{x}, t) dx dt, \end{aligned}$$

where  $\Sigma_n := \Omega \times J_n$  and  $dy dt$  is the differential element on the space-time boundary  $\partial\Omega \times J_n$  and

$$(1.7) \quad w(\mathbf{x}, t_{n-1}^+) := \lim_{t \rightarrow t_{n-1}^+} w(\mathbf{x}, t)$$

takes into account the fact that  $w(\mathbf{x}, t)$  is discontinuous in time at time  $t_{n-1}$ .

## 1.3 Characteristics

We define the characteristic  $\mathbf{y}(s; \mathbf{x}, t)$  passing through  $(\mathbf{x}, t)$ ,  $t \in J_n$  by the following initial value problem of the ordinary differential equation:

$$(1.8) \quad \begin{cases} \frac{d\mathbf{y}}{ds} = \frac{\mathbf{V}(\mathbf{y}, s)}{K(\mathbf{y}, s)} \\ \mathbf{y}(s; \mathbf{x}, t)|_{s=t} = \mathbf{x} \end{cases}$$

The notation  $\mathbf{y}(s; \mathbf{x}, t)$  can refer to tracking either forward or backward. In particular, we define

$$(1.9) \quad \mathbf{x}^* = \mathbf{y}(t_{n-1}; \mathbf{x}, t_n),$$

$$(1.10) \quad \tilde{\mathbf{x}} = \mathbf{y}(t_n; \mathbf{x}, t_{n-1}).$$

In other words,  $(\mathbf{x}, t_n)$  backtracks to  $(\mathbf{x}^*, t_{n-1})$  while  $(\mathbf{x}, t_{n-1})$  tracks forward to  $(\tilde{\mathbf{x}}, t_n)$ .

In numerical schemes, an exact tracking of characteristics is preferred whenever possible. If exact tracking is impossible, Euler quadrature or Runge-Kutta quadrature with multiple micro time steps within a global time step are often used.

Note that in many applications, (1.1) is usually coupled with an potential or pressure equation whose solution is often obtained via the mixed finite element method. For example, a Raviart-Thomas space is often used for the velocity field, which is calculated on the interfaces of each cell. With each cell, one component is piecewise linear in  $x$  and piecewise constant in  $y$ , while the other component is piecewise linear in  $y$  and piecewise constant in  $x$ .

## 1.4 Adjoint Equation

To eliminate the last term on the left-hand side of the variational form, we require the test functions satisfy the adjoint equation

$$(1.11) \quad w_t + \mathbf{V} \cdot \nabla w = 0.$$

Along characteristics the adjoint equation becomes an ordinary differential equation

$$\begin{cases} \frac{d}{ds} w(\mathbf{y}(s; \mathbf{x}, t), s) = 0, \\ w(\mathbf{y}(s; \mathbf{x}, t), s)|_{s=t} = w(\mathbf{x}, t), \end{cases}$$

which implies that test functions are constants along characteristics.

Choosing  $(\mathbf{x}, t) = (\mathbf{x}, t_n)$ , we see that once the test functions  $w(\mathbf{x}, t_n)$  are specified at time  $t_n$ , they are completely determined in the space-time strip  $\Omega \times J_n$ . Therefore, we obtain

$$\begin{aligned} & \int_{\Omega} u(\mathbf{x}, t_n) w(\mathbf{x}, t_n) d\mathbf{x} + \int_{J_n} \int_{\Omega} (\mathbf{D}\nabla u) \cdot \nabla w \, d\mathbf{x} dt \\ & \quad + \int_{J_n} \int_{\partial\Omega} (\mathbf{V}u - \mathbf{D}\nabla u) \cdot \mathbf{n} \, w \, dy dt \\ & = \int_{\Omega} u(\mathbf{x}, t_{n-1}) w(\mathbf{x}, t_{n-1}^+) d\mathbf{x} + \int_{J_n} \int_{\Omega} f(\mathbf{x}, t) w(\mathbf{x}, t) d\mathbf{x} dt, \end{aligned}$$

where the second term on the left-hand side is called diffusion term, the last term on the left-hand side is boundary term while last term on the right-hand side is source term.

## 1.5 Boundaries, Flows, and Tracking

Let  $\Gamma_n := \partial\Omega \times J_n$  and  $\Gamma_n^I, \Gamma_n^O, \Gamma_n^N$  be the inflow, outflow, and noflow space-time boundaries during time period  $J_n$  defined by

$$(1.12) \quad \begin{aligned} \Gamma_n^I &:= \{(\mathbf{x}, t) \mid \mathbf{x} \in \partial\Omega, t \in J_n, \mathbf{V}(\mathbf{x}, t) \cdot \mathbf{n}(\mathbf{x}) < 0\} \\ \Gamma_n^O &:= \{(\mathbf{x}, t) \mid \mathbf{x} \in \partial\Omega, t \in J_n, \mathbf{V}(\mathbf{x}, t) \cdot \mathbf{n}(\mathbf{x}) > 0\} \\ \Gamma_n^N &:= \{(\mathbf{x}, t) \mid \mathbf{x} \in \partial\Omega, t \in J_n, \mathbf{V}(\mathbf{x}, t) \cdot \mathbf{n}(\mathbf{x}) = 0\} \end{aligned}$$

To accurately measure the time period taken for a particle to move along a characteristic from the previous time step or the inflow boundary to the current time step or the outflow boundary, we introduce space-time (location-moment) dependent time steps.

For any  $\mathbf{x} \in \Omega$  and  $t = t_n$ , if the characteristic backtracks to a point within  $\Omega$  at time  $t_{n-1}$ , then we define

$$(1.13) \quad \Delta t^I(\mathbf{x}, t_n) = t_n - t_{n-1}.$$

If the characteristic backtracks to a point on the inflow boundary for some  $t^* \in (t_{n-1}, t_n]$ , then we define

$$(1.14) \quad \Delta t^I(\mathbf{x}, t_n) = t_n - t^*.$$

Similarly, for any  $(\mathbf{y}, t) \in \Gamma_n^O$ , we define

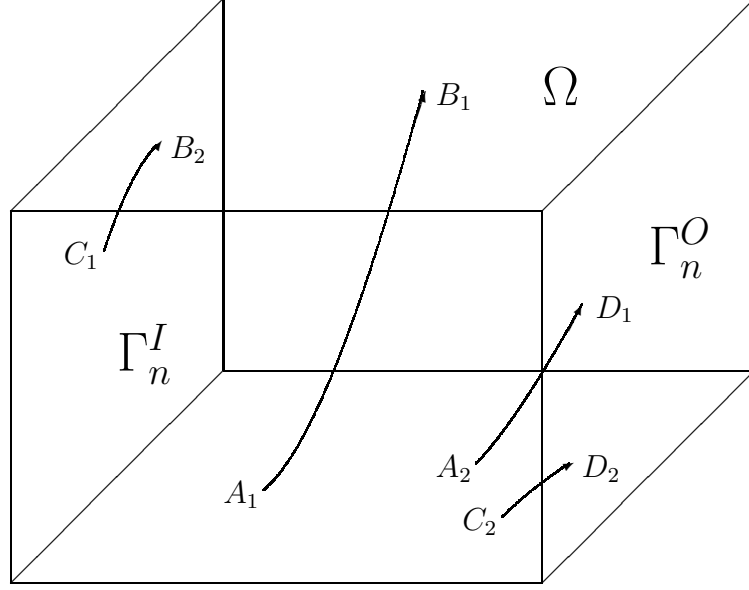
$$(1.15) \quad \Delta t^O(\mathbf{y}, t) = t - t_{n-1}$$

if the characteristic backtracks to within  $\Omega$  at time  $t_{n-1}$  or

$$(1.16) \quad \Delta t^O(\mathbf{y}, t) = t - t^*$$

if the characteristic backtracks to the inflow boundary at time  $t^* \in (t_{n-1}, t)$ .

Figure 1.1 might be helpful for understanding the above ideas. Assume that the left and front faces of the cube are inflow boundaries during time period  $J_n$  and the right and back faces are outflow space-time boundaries. Of course,  $\Omega$  at time  $t_{n-1}$  and  $\Omega$  at time  $t_n$  can be viewed as inflow and outflow boundaries, respectively. Furthermore, suppose  $A_1, A_2$  are in  $\Omega$  at time  $t_{n-1}$ ,  $B_1, B_2$  are in  $\Omega$  at time  $t_n$ ,  $C_1, C_2$  are on the inflow boundary  $\Gamma_n^I$ , and  $D_1, D_2$  are on the outflow boundary  $\Gamma_n^O$ . So we use  $\Delta t^I$  to measure streamlines  $A_1B_1, C_1B_2$  (of course  $\Delta t^I = \Delta t_n$  for  $A_1B_1$ ) and  $\Delta t^O$  to measure streamlines  $A_2D_1, C_2D_2$ .

Figure 1.1: *Flows, characteristics, and boundaries*

## 1.6 Approximations of Diffusion and Source Terms

Let  $\Sigma_n := \Omega \times J_n$  and  $\Sigma_n^O$  be the set of points in  $\Sigma_n$  that will flow out through  $\Gamma_n^O$  during time period  $J_n$ . By enforcing backward Euler quadrature at the current time  $t_n$  and on the outflow space-time boundary  $\Gamma_n^O$ , we get

$$\begin{aligned}
 & \int_{\Sigma_n} f(\mathbf{x}, t) w(\mathbf{x}, t) d\mathbf{x} dt \\
 &= \int_{\Sigma_n \setminus \Sigma_n^O} f(\mathbf{x}, t) w(\mathbf{x}, t) d\mathbf{x} dt + \int_{\Sigma_n^O} f(\mathbf{x}, t) w(\mathbf{x}, t) d\mathbf{x} dt \\
 &= \int_{\Omega} \Delta t^I(\mathbf{x}, t_n) f(\mathbf{x}, t_n) w(\mathbf{x}, t_n) d\mathbf{x} \\
 &\quad + \int_{\Gamma_n^O} \Delta t^O(\mathbf{y}, t) f(\mathbf{y}, t) w(\mathbf{y}, t) (\mathbf{V} \cdot \mathbf{n}) d\mathbf{y} dt \\
 (1.17) \quad &+ E(f, w).
 \end{aligned}$$

Similarly, the diffusion term can be approximated as follows

$$\begin{aligned}
& \int_{\Sigma_n} ((\mathbf{D}\nabla u) \cdot \nabla w)(\mathbf{x}, t) d\mathbf{x} dt \\
&= \int_{\Omega} \Delta t^I(\mathbf{x}, t_n) ((\mathbf{D}\nabla u) \cdot \nabla w)(\mathbf{x}, t_n) d\mathbf{x} \\
&\quad + \int_{\Gamma_n^O} \Delta t^O(\mathbf{y}, t) ((\mathbf{D}\nabla u) \cdot \nabla w)(\mathbf{y}, t) (\mathbf{V} \cdot \mathbf{n}) d\mathbf{y} dt \\
(1.18) \quad & + E(D, u, w).
\end{aligned}$$

## 1.7 Decomposition of Boundary Term

Notice that on noflow boundary, the total flux vanishes,

$$(1.19) \quad (\mathbf{V}u - \mathbf{D}\nabla u) \cdot \mathbf{n} \equiv 0,$$

so the boundary term can be further decomposed into two parts:

$$\begin{aligned}
& \int_{\Gamma_n} (\mathbf{V}u - \mathbf{D}\nabla u) \cdot \mathbf{n} w(\mathbf{y}, t) d\mathbf{y} dt \\
(1.20) \quad &= \int_{\Gamma_n^I} (\mathbf{V}u - \mathbf{D}\nabla u) \cdot \mathbf{n} w(\mathbf{y}, t) d\mathbf{y} dt \\
&\quad + \int_{\Gamma_n^O} (\mathbf{V}u - \mathbf{D}\nabla u) \cdot \mathbf{n} w(\mathbf{y}, t) d\mathbf{y} dt.
\end{aligned}$$

More details on handling these two boundary terms will be provided later.

## 1.8 Reference Equation

Dropping the error terms in the source and diffusion terms, we finally obtain the following reference equation:

Find  $u(\mathbf{x}, t) \in H^1(\Omega \times (t_{n-1}, t_n])$  so that the following holds for any  $w(\mathbf{x}, t) \in H^1(\Omega \times (t_{n-1}, t_n])$

$$\begin{aligned}
 & \int_{\Omega} u(\mathbf{x}, t_n) w(\mathbf{x}, t_n) d\mathbf{x} \\
 & + \int_{\Omega} \Delta t^I(\mathbf{x}, t_n) ((\mathbf{D}\nabla u) \cdot \nabla w)(\mathbf{x}, t_n) d\mathbf{x} \\
 & + \int_{\Gamma_n^O} \Delta t^O(\mathbf{y}, t) ((\mathbf{D}\nabla u) \cdot \nabla w)(\mathbf{V} \cdot \mathbf{n}) dy dt \\
 & + \int_{\Gamma_n^O} (\mathbf{V}u - \mathbf{D}\nabla u) \cdot \mathbf{n} w(\mathbf{y}, t) dy dt \\
 (1.21) \quad & = \int_{\Omega} u(\mathbf{x}^*, t_{n-1}) w(\mathbf{x}, t_n) \mathbf{J}(\mathbf{x}^*, \mathbf{x}) d\mathbf{x} \\
 & + \int_{\Omega} \Delta t^I(\mathbf{x}, t_n) f(\mathbf{x}, t_n) w(\mathbf{x}, t_n) d\mathbf{x} \\
 & + \int_{\Gamma_n^O} \Delta t^O(\mathbf{y}, t) f(\mathbf{y}, t) w(\mathbf{y}, t) (\mathbf{V} \cdot \mathbf{n}) dy dt \\
 & - \int_{\Gamma_n^I} (\mathbf{V}u - \mathbf{D}\nabla u) \cdot \mathbf{n} w(\mathbf{y}, t) dy dt,
 \end{aligned}$$

where  $\mathbf{x}^* := \mathbf{y}(t_{n-1}; \mathbf{x}, t_n)$  and  $\mathbf{J}(\mathbf{x}^*, \mathbf{x})$  is the Jacobian.

## Chapter 2

# Finite Element Methods within ELLAM Framework

One advantage of the ELLAM formulation is that there is basically no restriction on spatial discretizations. This leaves the door open for finite element methods and other methods, e.g., wavelet methods . For now, we choose trial functions and test functions from the standard finite element methods to develop numerical schemes for boundary initial value problems.

The main advantage and also the major difficulty of the ELLAM method is characteristic tracking. Actually there is no any restriction on the spatial domain in the ELLAM formulation. The main difficulty lies in locating the foot or head of a characteristic. Clearly, rectangular meshes offer a great deal of convenience for the locating mentioned above. So from now on we shall focus rectangular domains and hence rectangular meshes.

### 2.1 Partitions of Spatial Domain and Outflow Space-Time Boundary and Courant Number

Note that in the ELLAM formulation, the unknown function is defined on both  $\Omega$  at time  $t_n$  and the outflow space-time boundary  $\Gamma_n^O$ . This is in contrast to most numerical schemes for time-dependent problems, in which the unknown is typically defined only on the spatial domain  $\Omega$  at time  $t_n$ .

We first define a quasi-uniform spatial partition  $\mathcal{T}_h$  of mesh size  $h$  for domain  $\Omega$  at time  $t_n$ , then extend it to  $\Gamma_n^O$ .

During time period  $J_n$ , some of the mass on domain  $\Omega$  at time  $t_{n-1}$  will flow out through the outflow space-time boundary  $\Gamma_n^O$ . The number of spatial degrees of freedom crossing  $\Gamma_n^O$  is essentially the Courant number in the normal direction. To preserve this information, one should partition  $\Gamma_n^O$  in time direction with about the same number of subintervals. In other words, the local time partition on  $\Gamma_n^O$  should satisfy the CFL condition.

The ELLAM formulation uses Lagrangian coordinates and thus is not subject to the CFL restriction. However, on the outflow space-time boundary  $\Gamma_n^O$ , the temporal discretization should obey the CFL condition for the reason of accuracy and stability.

To be specific, we define Courant number on the outflow space-time boundary  $\Gamma_n^O$  by

$$(2.1) \quad Cr := \max_{(\mathbf{y}, t) \in \Gamma_n^O} |\mathbf{V}(\mathbf{y}, t) \cdot \mathbf{n}(\mathbf{y})| \frac{\Delta t_n}{h}$$

and  $NC$  as the ceiling of  $Cr$ . Then we define a uniform temporal partition on  $\Gamma_n^O$  by

$$(2.2) \quad t_{n,k} := t_n - k \frac{\Delta t_n}{NC}, \quad k = 0, 1, \dots, NC.$$

Finally, we extend the spatial partition  $\mathcal{T}_h$  on  $\Omega$  at time  $t_n$  to  $\Gamma_n^O$  with local time refinement given by (2.2). The united partition will be denoted by  $\mathcal{T}_{h,\Delta t}$ .

## 2.2 Two Groups of Trial and Test Functions

Note that in the reference equation (1.21), not all terms appear simultaneously. The first two terms on the left-hand side and the second term on the right-hand side correspond to only the test functions defined on  $\Omega$  at time  $t_n$ , the third and fourth terms on the left-hand side and the third term on the right-hand side correspond to only the test functions defined on the outflow space-time boundary  $\Gamma_n^O$ , while the last term on the left-hand side and the first term on the right-hand side correspond to possibly both.

So there are two groups of terms and equations. One group is related to the trial and test functions defined on  $\Omega$  at time  $t_n$ , the other corresponds to the trial and test functions defined on the outflow space-time boundary  $\Gamma_n^O$ .

These two groups of equations might be coupled or decoupled, depending on proposed boundary conditions.

## 2.3 Interior Nodes and Noflow Boundary

For any test function  $w$ , let  $\text{supp}(w)$  be its support on domain  $\Omega$  or the outflow boundary  $\Gamma_n^O$ , and  $\Sigma_w^*$  be the prism obtained by backtracking  $\text{supp}(w)$  along characteristics from  $\Omega$  at time  $t_n$  or  $\Gamma_n^O$  to  $\Omega$  at time  $t_{n-1}$  or the inflow boundary  $\Gamma_n^I$ .

If the test function  $w$  is defined on  $\Omega$  at time  $t_n$  and  $\Sigma_w^*$  does not intersect the inflow boundary  $\Gamma_n^I$  during time period  $J_n$ , then we obtain the following equations:

$$\begin{aligned}
 & \int_{\Omega} U(\mathbf{x}, t_n) w(\mathbf{x}, t_n) d\mathbf{x} \\
 & \quad + \int_{\Omega} \Delta t ((\mathbf{D}\nabla U) \cdot \nabla w)(\mathbf{x}, t_n) d\mathbf{x} \\
 (2.3) \quad & = \int_{\Omega} U(\mathbf{x}, t_{n-1}) w(\mathbf{x}, t_{n-1}^+) d\mathbf{x} \\
 & \quad + \int_{\Omega} \Delta t f(\mathbf{x}, t_n) w(\mathbf{x}, t_n) d\mathbf{x}.
 \end{aligned}$$

This implies that if all boundaries are noflow or all nodes are interior nodes, then the coefficient matrix of the whole system is 9-banded, symmetric and positive definite.

## 2.4 Inflow Boundary Conditions

No matter the test function is defined on  $\Omega$  at time  $t_n$  or on the outflow space-time boundary  $\Gamma_n^O$ , we have to deal with the inflow boundary term

$$(2.4) \quad \int_{\Gamma_n^I} (\mathbf{V}u - \mathbf{D}\nabla u) \cdot \mathbf{n} w(\mathbf{y}, t) dS$$

once  $\Sigma_w^*$  intersects  $\Gamma_n^I$ .

For a **inflow Robin (total flux) condition**, it becomes

$$(2.5) \quad \int_{\Gamma_n^I} (\mathbf{V}u - \mathbf{D}\nabla u) \cdot \mathbf{n} w(\mathbf{y}, t) dS = - \int_{\Gamma_n^I} g_3^I w(x, y, t) d\mathbf{y} dt$$

and can be moved to the right-hand side of the reference equation.

When we backtrack the support of a test function, its image is splitted into two parts, one in  $\Omega$  at time  $t_{n-1}$  and the other on the inflow space-time boundary  $\Gamma_n^I$ . Note that the factor  $\Delta t^I(\mathbf{x}, t_n)$  in the second term or  $\Delta t^I(\mathbf{y}, t_n)$  in the third term of the left-hand side is smaller than  $\Delta t_n$ . Nevertheless, the system still has a 9-banded, symmetric positive definite coefficient matrix.

For a **inflow Dirichlet condition**, the function values of  $u$  are known on the inflow space-time boundary  $\Gamma_n^I$ , and so are the tangential derivatives. But its normal derivatives are unknown on  $\Gamma_n^I$ . This means the unknown boundary diffusive flux is coupled with unknown interior function values. To resolve the problem, we approximate  $\nabla U(\mathbf{y}, t)$  on the inflow boundary  $\Gamma_n^I$  implicitly by  $\nabla U(\mathbf{x}(t_n; \mathbf{y}, t), t_n)$ . This removes the difficulty of evaluating an unknown diffusive boundary flux. The error is small since it is along characteristics. Be aware that this term introduces **nonsymmetry** to the coefficient matrix near the inflow boundary.

For a **inflow Neumann condition**, readers are referred to [6].

## 2.5 Outflow Boundary Conditions

Outflow boundary conditions involve the third term

$$(2.6) \quad \int_{\Gamma_n^O} \Delta t^O(\mathbf{y}, t) ((\mathbf{D}\nabla u) \cdot \nabla w)(\mathbf{y}, t) (\mathbf{V} \cdot \mathbf{n}) dS$$

and the fourth term

$$(2.7) \quad \int_{\Gamma_n^O} (\mathbf{V}u - \mathbf{D}\nabla u) \cdot \mathbf{n} w(\mathbf{y}, t) dS$$

on the left-hand side of the reference equation.

For a **outflow Dirichlet condition**, the function  $u$  and hence its tangential derivatives are known on the outflow space-time boundary  $\Gamma_n^O$ . Only the normal derivatives of the trial function  $U$  are taken as unknowns. But

their equations are decoupled from those associated with the values of the trial function  $U$  at interior nodes and are needed only for mass conservation. Therefore we omitt them here.

For a **outflow Neumann condition** or a **Outflow Robin condition**, some techniques have been successfully developed in [6].

## 2.6 FEM Assembly

FEM assembly

$$\begin{aligned}
 & \sum_E \int_E \left[ K(\mathbf{x}, t_n) u(\mathbf{x}, t_n) w(\mathbf{x}, t_n) + \Delta t^I(\mathbf{x}, t_n) ((\mathbf{D}\nabla u) \cdot \nabla w)(\mathbf{x}, t_n) \right] d\mathbf{x} \\
 & \quad + \int_{\Gamma_n^O} \left[ \Delta t^O(\mathbf{y}, t) ((\mathbf{D}\nabla u) \cdot \nabla w) (\mathbf{V} \cdot \mathbf{n}) \right. \\
 & \quad \quad \left. + (\mathbf{V}u - \mathbf{D}\nabla u) \cdot \mathbf{n} w(\mathbf{y}, t) \right] d\mathbf{y} dt \\
 (2.8) \quad & = \sum_E \int_E \left[ K(\mathbf{x}, t_{n-1}) u(\mathbf{x}^*, t_{n-1}) w(\mathbf{x}, t_n) \mathbf{J}(\mathbf{x}^*, \mathbf{x}) \right. \\
 & \quad \left. + \Delta t^I(\mathbf{x}, t_n) f(\mathbf{x}, t_n) w(\mathbf{x}, t_n) \right] d\mathbf{x} \\
 & \quad + \int_{\Gamma_n^O} \Delta t^O(\mathbf{y}, t) f(\mathbf{y}, t) w(\mathbf{y}, t) (\mathbf{V} \cdot \mathbf{n}) d\mathbf{y} dt \\
 & \quad - \int_{\Gamma_n^I} (\mathbf{V}u - \mathbf{D}\nabla u) \cdot \mathbf{n} w(\mathbf{y}, t) d\mathbf{y} dt,
 \end{aligned}$$

where  $\mathbf{x}^* := \mathbf{y}(t_{n-1}; \mathbf{x}, t_n)$  and  $\mathbf{J}(\mathbf{x}^*, \mathbf{x})$  is the Jacobian.



# Chapter 3

## Implementation

### 3.1 Assumptions on Problem and Method

Our implementation makes the following assumptions:

1. We consider a single-phase linear transport equation. If the velocity, diffusion, or reaction has mild nonlinearity, then the usual linearization should be OK.
2. The fluid velocity  $\mathbf{V}(\mathbf{x}, t)$  is assumed to be known. It might be obtained from another program. As will be discussed later, the velocity field affects characteristic tracking to a great deal.
3. At present, we have not included the reaction term. When the reaction term is included, we shall use the points on characteristics to evaluate  $\exp\left(-\int_{t_n}^{t^*} R(\mathbf{y}, s)ds\right)$ . This requires certain accuracy in characteristic tracking and small global time steps.
4. We assume a rectangular domain  $\Omega$  with a rectangular mesh parallel to the axes. Again this is mainly for convenience in characteristic tracking. A polygonal domain with a triangular mesh or even an unstructured mesh is not a hurdle to FEM assembly. Characteristic tracking in such a mesh is fairly complicated but is now under our investigation.
5. We shall use  $Q_1$  element on rectangles. Numerical experiments indicate that the  $h$ -version convergence suffices.

6. The current version is for 2-dim problems, but will be extended into a dimension-independent version in the near future.
7. We further assume the retardation, diffusion, and source terms are constants on each element, respectively. Therefore, computations of the element mass and stiffness matrices and the source right-hand side will be greatly simplified. Usually elements are small and the above quantities do not experience big changes in a small element, so resulting errors should be small also.
8. Computing the mass contribution from the domain at the previous time step involves the Jacobian of characteristic tracking, which is of order  $1 + \mathcal{O}(\Delta t)$ . For simplicity, we shall use the Jacobian of the Euler method, even though Euler, Runge-Kutta, or other methods could be used for the actual tracking.

## 3.2 FEM Assembly

FEM assembly

$$\begin{aligned}
 & \sum_E \int_E \left[ K(\mathbf{x}, t_n) u(\mathbf{x}, t_n) w(\mathbf{x}, t_n) + \Delta t^I(\mathbf{x}, t_n) ((\mathbf{D}\nabla u) \cdot \nabla w)(\mathbf{x}, t_n) \right] d\mathbf{x} \\
 & \quad + \int_{\Gamma_n^O} \left[ \Delta t^O(\mathbf{y}, t) ((\mathbf{D}\nabla u) \cdot \nabla w)(\mathbf{V} \cdot \mathbf{n}) \right. \\
 & \quad \quad \left. + (\mathbf{V}u - \mathbf{D}\nabla u) \cdot \mathbf{n} w(\mathbf{y}, t) \right] dy dt \\
 (3.1) \quad & = \sum_E \int_E \left[ K(\mathbf{x}, t_{n-1}) u(\mathbf{x}^*, t_{n-1}) w(\mathbf{x}, t_n) \mathbf{J}(\mathbf{x}^*, \mathbf{x}) \right. \\
 & \quad \left. + \Delta t^I(\mathbf{x}, t_n) f(\mathbf{x}, t_n) w(\mathbf{x}, t_n) \right] d\mathbf{x} \\
 & \quad + \int_{\Gamma_n^O} \Delta t^O(\mathbf{y}, t) f(\mathbf{y}, t) w(\mathbf{y}, t) (\mathbf{V} \cdot \mathbf{n}) dy dt \\
 & \quad - \int_{\Gamma_n^I} (\mathbf{V}u - \mathbf{D}\nabla u) \cdot \mathbf{n} w(\mathbf{y}, t) dy dt,
 \end{aligned}$$

where  $\mathbf{x}^* := \mathbf{y}(t_{n-1}; \mathbf{x}, t_n)$  and  $\mathbf{J}(\mathbf{x}^*, \mathbf{x})$  is the Jacobian.

### 3.3 Mesh and Timing

Actually, there is only one time step in the ELLAM methodology: from time  $t_{n-1}$  to time  $t_n$ . It assumes we have knowledge about  $u$  on  $\Omega$  at  $t_{n-1}$  and on the inflow boundary  $\partial\Omega$  during  $[t_{n-1}, t_n]$ , then solve for the solution on  $\Omega$  at time  $t_n$  and the outflow boundary.

The domain  $\Omega$  can be discretized into a rectangular mesh, or a triangular mesh, or an even mixed (unstructured) one, whatsoever makes sense. The mesh does not change during time stepping.

But we also need a partition for the outflow boundary  $\Gamma_n^O$ , which is a tensor product of the partition on  $\partial\Omega$  and a partition of  $J_n = [t_{n-1}, t_n]$ . As was discussed before, any partition of  $J_n$  should satisfy the CFL condition.

Now we have two groups of unknowns on  $\Omega_n$  and  $\Gamma_n^O$ , respectively, and two groups of trial/test functions and hence two groups of equations. The formulation of equations for each group is normal, but the assembly of these two groups needs some extra effort.

- Mesh for  $\Omega$ ;
- Mesh on  $\Gamma_n^O$ ;
- Trial/test functions, equations for  $\Omega_n$ ;
- Trial/test functions, equations for  $\Gamma_n^O$ ;
- Assembly of these two groups of equations

### 3.4 Numerical Integration

As was seen in the previous sections, ELLAM involves numerical integrations on finite elements. We can apply the trapezoid, Simpson, Gaussian 1-, 2-, 3-, 5- point quadrature on the standard interval  $[-1, 1]$ .

Suppose we have two standard quadratures QuadX, QuadY on the interval  $[-1, 1]$  and they are used for numerical integrations on the rectangular element with corners  $(x_0, y_0), (x_1, y_1)$ . The quadrature QuadX has  $N_x$  quadrature points  $X_i, (0 \leq i < N_x)$  and the quadrature QuadY has  $N_y$

quadrature points  $Y_j$ , ( $0 \leq j < N_y$ ), respectively. Applying the following 2 mappings from  $[x_0, x_1]$  or  $[y_0, y_1]$  to  $[-1, 1]$ ,

$$x = \frac{x_1 - x_0}{2}X + \frac{x_1 + x_0}{2}, \quad -1 \leq X \leq 1,$$

$$y = \frac{y_1 - y_0}{2}Y + \frac{y_1 + y_0}{2}, \quad -1 \leq Y \leq 1,$$

we can easily find the corresponding integration points in the intervals  $[x_0, x_1]$  and  $[y_0, y_1]$ .

### 3.5 Matrices for the Reference Element

For a 2-dim rectangular mesh, all elements can be mapped back to the reference element: the unit square  $[0, 1] \times [0, 1]$ . Accordingly, their nodal basis functions and gradients can be expressed in terms of the nodal basis functions on the reference element. So let us work on the reference element first.

Table 3.1: Frequently used standard quadratures

name	NumPts	point	weight
trapezoid	2	-1.0	1.0
		1.0	1.0
Simpson	3	-1.0	0.333,333,333,333
		0.0	1.333,333,333,334
		1.0	0.333,333,333,333
Gaussian1	1	0.0	2
Gaussian2	2	-0.577,350,269,2??	1.0
		0.577,350,269,2??	1.0
Gaussian3	3	-0.774,596,669,2??	0.555,555,555,556
		0.0	0.888,888,888,889
		0.774,596,669,2??	0.555,555,555,556
Gaussian5	5	-0.906,179,845,939	0.236,926,885,056
		-0.538,469,310,106	0.478,628,670,499
		0.0	0.568,888,888,889
		0.538,469,310,106	0.478,628,670,499
		0.906,179,845,939	0.236,926,885,056

### 3.5.1 Mass Matrix for the Reference Element

Let  $\Phi_m(X, Y)$ , ( $m = 0, 1, 2, 3$ ) (or 00, 01, 10, 11 in binary digits) be the  $\mathcal{Q}_1$  nodal basis functions corresponding to the nodes  $(0, 0)$ ,  $(0, 1)$ ,  $(1, 0)$ ,  $(1, 1)$  of the reference element. Then we have

$$(3.2) \quad \begin{aligned} \Phi_0 &= \Phi_{00} = (1 - X)(1 - Y), \\ \Phi_1 &= \Phi_{01} = (1 - X)Y, \\ \Phi_2 &= \Phi_{10} = X(1 - Y), \\ \Phi_3 &= \Phi_{11} = XY. \end{aligned}$$

These are the local trial and test functions on the reference element. The mass matrix for the reference element, which can be calculated exactly (without using any quadrature), is

$$(3.3) \quad M = [\langle \Phi_{m_1}, \Phi_{m_2} \rangle] = \begin{bmatrix} \frac{1}{9} & \frac{1}{18} & \frac{1}{18} & \frac{1}{36} \\ \frac{1}{18} & \frac{1}{9} & \frac{1}{36} & \frac{1}{18} \\ \frac{1}{18} & \frac{1}{36} & \frac{1}{9} & \frac{1}{18} \\ \frac{1}{36} & \frac{1}{18} & \frac{1}{18} & \frac{1}{9} \end{bmatrix} = \frac{1}{36} \begin{bmatrix} 4 & 2 & 2 & 1 \\ 2 & 4 & 1 & 2 \\ 2 & 1 & 4 & 2 \\ 1 & 2 & 2 & 4 \end{bmatrix}$$

All the functions are of product type, so we only need to evaluate integrals like

$$\int_0^1 s^2 ds = \int_0^1 (1 - s)^2 ds = \frac{1}{3} \quad \text{and} \quad \int_0^1 s(1 - s) ds = \frac{1}{6}.$$

### 3.5.2 Stiffness Matrix for the Reference Element

For the gradients, we have

$$(3.4) \quad \begin{aligned} \nabla \Phi_0 &= [-(1 - Y), -(1 - X)], \\ \nabla \Phi_1 &= [-Y, 1 - X], \\ \nabla \Phi_2 &= [1 - Y, -X], \\ \nabla \Phi_3 &= [Y, X]. \end{aligned}$$

Then the reference element stiffness matrix is

$$(3.5) \quad S = \left[ \int_0^1 \int_0^1 \nabla \Phi_{m_1} \cdot \nabla \Phi_{m_2} dXdY \right] = [ \text{something} ]$$

Note that we have

$$[(\Phi_0)_X, (\Phi_1)_X, (\Phi_2)_X, (\Phi_3)_X] = [-(1 - Y), -Y, 1 - Y, Y]$$

and

$$[(\Phi_0)_Y, (\Phi_1)_Y, (\Phi_2)_Y, (\Phi_3)_Y] = [-(1 - X), 1 - X, -X, X].$$

So the stiffness matrix  $S$  can be split into 2 parts as  $S = S_X + S_Y$  with

$$(3.6) \quad S_X = \begin{bmatrix} \frac{1}{3} & \frac{1}{6} & -\frac{1}{3} & -\frac{1}{6} \\ \frac{1}{6} & \frac{1}{3} & -\frac{1}{6} & -\frac{1}{3} \\ -\frac{1}{3} & -\frac{1}{6} & \frac{1}{3} & \frac{1}{6} \\ -\frac{1}{6} & -\frac{1}{3} & \frac{1}{6} & \frac{1}{3} \end{bmatrix} = \frac{1}{6} \begin{bmatrix} 2 & 1 & -2 & -1 \\ 1 & 2 & -1 & -2 \\ -2 & -1 & 2 & 1 \\ -1 & -2 & 1 & 2 \end{bmatrix}$$

and

$$(3.7) \quad S_Y = \frac{1}{6} \begin{bmatrix} 2 & -2 & 1 & -1 \\ -2 & 2 & -1 & 1 \\ 1 & -1 & 2 & -2 \\ -1 & 1 & -2 & 2 \end{bmatrix}.$$

### 3.5.3 Source RHS for the Reference Element

Assume the source term  $f(x, y) \equiv 1$  on the reference element, then we have

$$(3.8) \quad \text{RHS} = \frac{1}{4} \begin{bmatrix} 1 \\ 1 \\ 1 \\ 1 \end{bmatrix},$$

whence we compute integrals like

$$\int_0^1 s ds = \int_0^1 (1 - s) ds = \frac{1}{4}.$$

## 3.6 Matrices on General Elements

Now we compute the mass and stiffness matrices on a general rectangular element with corner points  $(x_0, y_0)$  and  $(x_1, y_1)$ . Let  $\varphi_m(x, y)$ ,  $(m = 0, 1, 2, 3)$  (or 00, 01, 10, 11 in binary digits) be the  $\mathcal{Q}_1$  nodal basis functions corresponding to its nodes  $(x_0, y_0)$ ,  $(x_0, y_1)$ ,  $(x_1, y_0)$ ,  $(x_1, y_1)$ . Applying the following coordinate transforms,

$$(3.9) \quad \begin{aligned} x &= (x_1 - x_0)X + x_0, & 0 \leq X \leq 1, \\ y &= (y_1 - y_0)Y + y_0, & 0 \leq Y \leq 1, \end{aligned}$$

we get

$$\varphi_m(x, y) = \Phi_m(X, Y).$$

For convenience, let us denote  $x_l = x_1 - x_0$ ,  $y_l = y_1 - y_0$ .

### 3.6.1 Mass Matrix

Based on the above changes of variables, we obtain

$$(3.10) \quad M = x_l y_l \frac{1}{36} \begin{bmatrix} 4 & 2 & 2 & 1 \\ 2 & 4 & 1 & 2 \\ 2 & 1 & 4 & 2 \\ 1 & 2 & 2 & 4 \end{bmatrix}$$

### 3.6.2 Stiffness Matrix

First we have

$$\frac{\partial}{\partial x} \varphi_m(x, y) = \frac{\partial \Phi_m(X, Y)}{\partial X} \frac{dX}{dx} = \frac{\partial \Phi_m(X, Y)}{\partial X} \frac{1}{x_l}.$$

Similarly,

$$\frac{\partial}{\partial y} \varphi_m(x, y) = \frac{\partial \Phi_m(X, Y)}{\partial Y} \frac{1}{y_l}.$$

Then we have

$$\nabla \varphi_{m_1} \cdot \nabla \varphi_{m_2} = \frac{1}{x_l^2} \frac{\partial \Phi_{m_1}}{\partial X} \frac{\partial \Phi_{m_2}}{\partial X} + \frac{1}{y_l^2} \frac{\partial \Phi_{m_1}}{\partial Y} \frac{\partial \Phi_{m_2}}{\partial Y}$$

Further calculations indicate that

$$\int_{x_0}^{x_1} \int_{y_0}^{y_1} \nabla \varphi_{m_1} \cdot \nabla \varphi_{m_2} dx dy = \frac{y_l}{x_l} \int_0^1 \int_0^1 \frac{\partial \Phi_{m_1}}{\partial X} \frac{\partial \Phi_{m_2}}{\partial X} dX dY + \frac{x_l}{y_l} \int_0^1 \int_0^1 \frac{\partial \Phi_{m_1}}{\partial Y} \frac{\partial \Phi_{m_2}}{\partial Y} dX dY$$

Therefore the stiffness matrix have to be split into 2 parts:

$$S = \frac{y_l}{x_l} S_X + \frac{x_l}{y_l} S_Y$$

that is,

$$(3.11) \quad S = \frac{y_l}{x_l} \frac{1}{6} \begin{bmatrix} 2 & 1 & -2 & -1 \\ 1 & 2 & -1 & -2 \\ -2 & -1 & 2 & 1 \\ -1 & -2 & 1 & 2 \end{bmatrix} + \frac{x_l}{y_l} \frac{1}{6} \begin{bmatrix} 2 & -2 & 1 & -1 \\ -2 & 2 & -1 & 1 \\ 1 & -1 & 2 & -2 \\ -1 & 1 & -2 & 2 \end{bmatrix}.$$

### 3.6.3 Source RHS

Similarly,

$$(3.12) \quad \text{RHS} = \frac{x_l y_l}{4} \begin{bmatrix} 1 \\ 1 \\ 1 \\ 1 \end{bmatrix}$$



### 3.8 Linear Solvers

When a linear system is symmetric positive, we employ the conjugate gradient (CG) method as our linear solver, see [2] Algorithm 10.2.1 and flow chart (10.2.16). For the nonsymmetric case, we use GMRES instead.

In the following flow chart,  $\varepsilon$  is the (relative) tolerance and  $k_{\max}$  is the iteration maximum, other notations are self-explanatory.

```

 $k = 0$ 
 $x = \text{initial guess}$ 
 $r = b - Ax$ 
 $\gamma_0 = r^T r$ 
 $\text{res} = \sqrt{\gamma_0}$ 
 $\text{rhs} = \|b\|_2$ 
while ( $k < k_{\max}$ )  $\wedge$  ( $\text{res} > \varepsilon \text{ rhs}$ )
     $k = k + 1$ 
    if  $k = 1$ 
         $p = r$ 
    else
         $\beta = \gamma_{k-1} / \gamma_{k-2}$ 
         $p = r + \beta p$ 
    end
     $q = Ap$ 
     $\delta = p^T q$ 
     $\alpha = \gamma_{k-1} / \delta$ 
     $x = x + \alpha p$ 
     $r = r - \alpha q$ 
     $\gamma_k = r^T r$ 
     $\text{res} = \sqrt{\gamma_k}$ 
end

```

### 3.9 Characteristic Tracking

Characteristic tracking is a vital part of ELLAM and also an important aspect for many numerical methods in computational fluid mechanics, as of my knowledge. Both forward and backward tracking are used in ELLAM. Although ELLAM is not subject to the CFL conditions in terms of stability, time steps should not be too large for the sake of accuracy. Optimal time steps for given data with minimal regularities are discussed in [4]. Based on these considerations, we require the temporal partition on the outflow boundary to satisfy the CFL conditions. For a typical step in the ELLAM framework, backtracking of characteristics is carried out from the domain  $\Omega$  at time  $t_n$  or the outflow boundary  $\Gamma_n^O$  to the domain at  $t_{n-1}$  or the inflow boundary  $\Gamma_n^I$ . We shall use the same temporal partition on the outflow boundary for characteristic backtracking.

Mathematically, characteristic tracking is expressed as solving an initial value problem to an ODE

$$(3.13) \quad \begin{cases} \frac{d\mathbf{y}}{ds} = \mathbf{V}(\mathbf{y}, s) \\ \mathbf{y}(s; \mathbf{x}, t)|_{s=t} = \mathbf{x} \end{cases}$$

But it involves many aspects: a spatial domain  $\Omega$ , a time period  $[t_{n-1}, t_n]$ , an outflow boundary  $\Gamma_n^O$ , a velocity vector field defined on the prism  $\Sigma_n = \Omega \times [t_{n-1}, t_n]$ , the proposed numerical methods (e.g. Euler or Runge-Kutta methods) and (not so obviously) meshes on the domain and the outflow boundary. If the mesh used in ELLAM is a triangular mesh instead a rectangular one, then some efforts have to be spent on locating the feet of the characteristics. In more general cases, the velocity could be just a numerical solution produced by another numerical method and very likely defined on a different mesh of  $\Omega$ . Then we have to further locate the intermediate node after each micro step in characteristic tracking. At this stage of design, however, we assume the mesh used in ELLAM is a rectangular mesh and the velocity is a function defined on  $\Sigma_n = \Omega \times [t_{n-1}, t_n]$ .

The code for implementing characteristic tracking should be dimension-independent. Starting from the current position/moment, we march to the next position/moment. The operations performed are a velocity vector times a time increment (a scalar) (which gives a position shift) and an addition of two positions (point  $\mathbf{j} = \text{point} + \text{vector} * \text{scalar}$ ).

Characteristics make a perfect case for a class. We name it **chara**, since **char** is already taken by most programming languages.

### 3.10 Examples

**Example 0** The domain  $\Omega = [-1, 1]^2$ , the time period  $[t_0, t_f] = [0, 1]$ . The velocity  $\mathbf{v} = (a, b)$ , possibly  $(1, 1)$ ,  $(1, 0)$ , or  $(0, 1)$ . The diffusion  $D$  is a small positive constant. For simplicity, we assume there is no reaction term:  $R \equiv 0$ . The exact solution is specified as

$$u(x, y, t) = \exp\left(-\frac{(x - x_c - at)^2 + (y - y_c - bt)^2}{2\sigma^2}\right).$$

This is a moving Gaussian hill. The center  $(x_c + at, y_c + bt)$  should be well inside  $\Omega$  so that  $u$  is numerically zero on  $\partial\Omega$ . An initial condition is derived accordingly.

Here are some details:

$$u_t = \frac{a(x - x_c - at) + b(y - y_c - bt)}{\sigma^2}u.$$

The velocity is div-free:  $\nabla \cdot \mathbf{v} = 0$ . Furthermore,

$$u_x = -\frac{x - x_c - at}{\sigma^2}u, \quad u_y = -\frac{y - y_c - bt}{\sigma^2}u,$$

and

$$\mathbf{v} \cdot \nabla u = -\frac{a(x - x_c - at) + b(y - y_c - bt)}{\sigma^2}u,$$

hence

$$u_t + \nabla \cdot (\mathbf{v}u) = 0.$$

Moreover,

$$\Delta u = -\frac{2}{\sigma^2}u + \frac{(x - x_c - at)^2 + (y - y_c - bt)^2}{\sigma^4}u.$$

Therefore,

$$f(x, y, t) = \frac{2D}{\sigma^2}u - D\frac{(x - x_c - at)^2 + (y - y_c - bt)^2}{\sigma^4}u.$$

In numerical runs, we set  $D = 10^{-3}$ ,  $\sigma = 0.0894$  so that  $1/\sigma^2 = 62.5$ .

**Example 1** The domain  $\Omega = [-1, 1]^2$ . The velocity  $\mathbf{v} = (-4y, 4x)$  is incompressible, i.e.,  $\nabla \cdot \mathbf{v} = 0$ . The time period  $[t_0, t_f] = [0, \pi/2]$ , which is needed for one complete rotation. The characteristic with head  $(x, y, t)$  and foot  $(x^*, y^*, 0)$  satisfies

$$(3.14) \quad \begin{bmatrix} x^* \\ y^* \end{bmatrix} = \begin{bmatrix} \cos(4t) & \sin(4t) \\ -\sin(4t) & \cos(4t) \end{bmatrix} \begin{bmatrix} x \\ y \end{bmatrix}.$$

An initial condition

$$(3.15) \quad u_0(x, y) = \exp\left(-\frac{(x - x_c)^2 + (y - y_c)^2}{2\sigma^2}\right)$$

is a Gaussian hill centered at  $(x_c, y_c)$ . The exact solution for the convection-diffusion equation with a constant diffusion  $D > 0$  and  $f = 0$  is

$$(3.16) \quad u(x, y, t) = \frac{2\sigma^2}{2\sigma^2 + 4Dt} \exp\left(-\frac{(x^* - x_c)^2 + (y^* - y_c)^2}{2\sigma^2 + 4Dt}\right),$$

where  $x^*, y^*$  are expressed in Equation (3.14). In our numerical experiment, we take  $D = 10^{-4}$ ,  $(x_c, y_c) = (-0.5, 0)$ , and  $\sigma = 0.0447$  so that  $2\sigma^2 = 0.0040$ . Then the maximum concentration at the final time  $t_f$  is 0.8642.



# Chapter 4

## Source Code of a Mini Version ELLAM

Here is the C++ code for a mini version ELLAM for the convection-diffusion equation on a uniform 2-dim rectangular mesh.

### 4.1 MiniELLAM: Head File

```
// MiniELLAM.h
// Jiangguo (James) Liu, ColoState, 12/2008 - 02/2009

class ELLAM {
public:
    ELLAM();
    ~ELLAM();
    void setMesh(double a, double b, double c, double d, int nx, int ny);
    void setTime(double t0, double tf, int nt);
    void setDiffConst(double ExDiff);
    void setVelFxnns(double(*ExVelx)(double x, double y, double t),
        double(*ExVely)(double x, double y, double t));
    void setSrsFxn(double(*ExSrs)(double x, double y, double t));
    void setVelData(double (*ExVx), double (*ExVy), int nx, int ny, int order);
    void setInitCond(double *U, int nx, int ny, int order);
    void getFinalSln(double *U, int nx, int ny, int order);
};
```

```

    void execute(int verbosity);
private:
    int NX, NY, NT;
    double XA, XB, YC, YD, T;
    double Deltax, Deltay, Deltat;
    double *X, *Y, *U0, *UT, *VX, *VY;
    double diff;
    double (*velx)(double x, double y, double t);
    double (*vely)(double x, double y, double t);
    double (*srs)(double x, double y, double t);
    void velxy(double &vx, double &vy, double x, double y, double t);
    void asmGlbMat(double *GlbMat, int *GlbMatNdx);
    void trknExEuler(double &xstar, double &ystar,
        double xn, double yn, double tn, double tn1);
    void asmGlbRHS4OldMass(double *GlbRHS, double *Un1, double tn);
    void asmGlbRHS4Srs(double *GlbRHS, double tn);
    void modGlbSysDirichletBndryCond(double *GlbMat, double *GlbRHS);
    int slvGlbSysBiCGStab(int n, double *x, double *A, int *M,
        double *b, double tol);
};

```

## 4.2 MiniELLAM: Source Code

```

// MiniELLAM.cpp
// Jiangguo (James) Liu, ColoState, 12/2008 - 02/2009

#include <cmath>
#include <iostream>
#include <stdio.h>
#include <stdlib.h>
#include "MiniELLAM.h"
using namespace std;

// The 3rd order Gaussian quadrature on  $[-1,1]^2$ 

```

```

static int GQR3npts = 9;
static double GQR3wab[9][3] = {
    0.07716049382716, -0.77459666924148, -0.77459666924148,
    0.12345679012346,  0.000000000000000, -0.77459666924148,
    0.07716049382716,  0.77459666924148, -0.77459666924148,
    0.12345679012346, -0.77459666924148,  0.000000000000000,
    0.19753086419753,  0.000000000000000,  0.000000000000000,
    0.12345679012346,  0.77459666924148,  0.000000000000000,
    0.07716049382716, -0.77459666924148,  0.77459666924148,
    0.12345679012346,  0.000000000000000,  0.77459666924148,
    0.07716049382716,  0.77459666924148,  0.77459666924148};

// ELLAM: default constructor

ELLAM::ELLAM()
{
    NX = 0;  NY = 0;  NT = 0;
    X = 0;  Y = 0;  U0 = 0;  UT = 0;  VX = 0;  VY = 0;  // Null pointers
    velx = 0;  vely = 0;  srs = 0;  // Null pointers to functions
}

// ELLAM: destructor

ELLAM::~~ELLAM()
{
    delete[] X, Y, U0, UT, VX, VY;
}

// ELLAM: setup a uniform rectangular mesh on a given rectangle

void ELLAM::setMesh(double a, double b, double c, double d,
    int nx, int ny)
{
    int i, j;

```

```
XA = a;  XB = b;  YC = c;  YD = d;
NX = nx;  NY = ny;

Deltax = (XB-XA)/NX;
Deltay = (YD-YC)/NY;

X = new double[NX+1];
Y = new double[NY+1];

X[0] = XA;
for (i=1; i<NX; ++i)  X[i] = X[i-1] + Deltax;
X[NX] = XB;

Y[0] = YC;
for (j=1; j<NY; ++j)  Y[j] = Y[j-1] + Deltay;
Y[NY] = YD;

return;
}

// ELLAM: setup a uniform time partition for marching

void ELLAM::setTime(double t0, double tf, int nt)
{
    T = tf - t0;  NT = nt;  Deltat = T/NT;
    return;
}

// ELLAM: set a positive diffusion constant

void ELLAM::setDiffConst(double ExDiff)
{
    diff = ExDiff;
    return;
}
```

```
// ELLAM: set velocity data on the mesh

void ELLAM::setVelData(double (*ExVx), double (*ExVy),
    int nx, int ny, int order)
{
    int k;

    if (nx!=NX || ny!=NY) {
        cout << "Mesh mismatch!\n";
        exit(-1);
    }

    VX = new double[(NX+1)*(NY+1)];
    VY = new double[(NX+1)*(NY+1)];

    if (order==0) {
        for (k=0; k<(NX+1)*(NY+1); ++k) {
            VX[k] = ExVx[k];
            VY[k] = ExVy[k];
        }
    }

    return;
}

// ELLAM: set the velocity functions in the PDE

void ELLAM::setVelFxn(double(*ExVelx)(double x, double y, double t),
    double(*ExVely)(double x, double y, double t))
{
    velx = ExVelx;
    vely = ExVely;
    return;
}
```

```

// ELLAM: set the source function in the PDE

void ELLAM::setSrsFxn(double(*ExSrs)(double x, double y, double t))
{
    srs = ExSrs;
    return;
}

// ELLAM: interpolation velocity function
// Bilinear interpolation of the discrete velocity data
// Given x, y, assuming steady (independent of t)
// Return vx, vy (passing by reference)

void ELLAM::velxy(double &vx, double &vy, double x, double y, double t)
{
    int i = (int)floor((x-XA)/Deltax);
    int j = (int)floor((y-YC)/Deltay);

    double x0 = X[i];
    double x1 = X[i+1];
    double y0 = Y[j];
    double y1 = Y[j+1];

    double w00 = ((x1-x)/(x1-x0)) * ((y1-y)/(y1-y0));
    double w10 = ((x-x0)/(x1-x0)) * ((y1-y)/(y1-y0));
    double w01 = ((x1-x)/(x1-x0)) * ((y-y0)/(y1-y0));
    double w11 = ((x-x0)/(x1-x0)) * ((y-y0)/(y1-y0));

    double VX00 = VX[j*(NX+1)+i];
    double VX10 = VX[j*(NX+1)+i+1];
    double VX01 = VX[(j+1)*(NX+1)+i];
    double VX11 = VX[(j+1)*(NX+1)+i+1];
    vx = VX00*w00 + VX10*w10 + VX01*w01 + VX11*w11;

    double VY00 = VY[j*(NX+1)+i];
    double VY10 = VY[j*(NX+1)+i+1];
    double VY01 = VY[(j+1)*(NX+1)+i];

```

```

double VY11 = VY[(j+1)*(NX+1)+i+1];
vy = VY00*w00 + VY10*w10 + VY01*w01 + VY11*w11;

return;
}

// ELLAM: assemble the global coefficient matrix
// GlbMatNdx: the auxiliary index matrix for the 9-banded coeff. matrix

void ELLAM::asmGlbMat(double *GlbMat, int *GlbMatNdx)
{
    // FILE *fp;
    int i, j, ie, je, k, l, nbr[4][4];
    int lblVrtx[4];
    double val, xel, yel;
    double RMM[4][4], RSMX[4][4], RSMY[4][4];
    double EMM[4][4], ESM[4][4], eltMat[4][4];

    // Reference Q1 element mass matrix (RMM)

    RMM[0][0] = 4;  RMM[0][1] = 2;  RMM[0][2] = 2;  RMM[0][3] = 1;
    RMM[1][0] = 2;  RMM[1][1] = 4;  RMM[1][2] = 1;  RMM[1][3] = 2;
    RMM[2][0] = 2;  RMM[2][1] = 1;  RMM[2][2] = 4;  RMM[2][3] = 2;
    RMM[3][0] = 1;  RMM[3][1] = 2;  RMM[3][2] = 2;  RMM[3][3] = 4;

    for (j=0; j<4; ++j)
        for (i=0; i<4; ++i)
            RMM[i][j] *= 1.0/36;

    // Reference Q1 element stiffness matrix -- X part (RSMX)

    RSMX[0][0] = 2;  RSMX[0][1] = 1;  RSMX[0][2] = -2;  RSMX[0][3] = -1;
    RSMX[1][0] = 1;  RSMX[1][1] = 2;  RSMX[1][2] = -1;  RSMX[1][3] = -2;
    RSMX[2][0] = -2; RSMX[2][1] = -1; RSMX[2][2] = 2;  RSMX[2][3] = 1;
    RSMX[3][0] = -1; RSMX[3][1] = -2; RSMX[3][2] = 1;  RSMX[3][3] = 2;

    for (j=0; j<4; ++j)

```

```

    for (i=0; i<4; ++i)
        RSMX[i][j] *= 1.0/6;

// Reference Q1 element stiffness matrix -- Y part (RSMY)

RSMY[0][0] = 2;  RSMY[0][1] = -2;  RSMY[0][2] = 1;  RSMY[0][3] = -1;
RSMY[1][0] = -2; RSMY[1][1] = 2;  RSMY[1][2] = -1; RSMY[1][3] = 1;
RSMY[2][0] = 1;  RSMY[2][1] = -1; RSMY[2][2] = 2;  RSMY[2][3] = -2;
RSMY[3][0] = -1; RSMY[3][1] = 1;  RSMY[3][2] = -2; RSMY[3][3] = 2;

for (j=0; j<4; ++j)
    for (i=0; i<4; ++i)
        RSMY[i][j] *= 1.0/6;

// Neighbors' column indices in the 9-band global matrix

nbr[0][0] = 4;  nbr[0][1] = 5;  nbr[0][2] = 7;  nbr[0][3] = 8;
nbr[1][0] = 3;  nbr[1][1] = 4;  nbr[1][2] = 6;  nbr[1][3] = 7;
nbr[2][0] = 1;  nbr[2][1] = 2;  nbr[2][2] = 4;  nbr[2][3] = 5;
nbr[3][0] = 0;  nbr[3][1] = 1;  nbr[3][2] = 3;  nbr[3][3] = 4;

// Setzero

for (k=0; k<(NX+1)*(NY+1); ++k) {
    for (l=0; l<9; ++l) {
        GlbMat[k*9+l] = 0.0;
        GlbMatNdx[k*9+l] = -1;
    }
}

// Assemble the global coefficient matrix

for (je=1; je<=NY; ++je) {
    yel = Y[je] - Y[je-1];
    for (ie=1; ie<=NX; ++ie) {
        xel = X[ie] - X[ie-1];
        for (j=0; j<4; ++j) {
            for (i=0; i<4; ++i) {

```

```

        EMM[i][j] = (xel*yel)*RMM[i][j];
        ESM[i][j] = (yel/xel)*RSMX[i][j] + (xel/yel)*RSMY[i][j];
        eltMat[i][j] = EMM[i][j] + (Deltat*diff)*ESM[i][j];
    }
}
lblVrtx[0] = (je-1)*(NX+1) + (ie-1);
lblVrtx[1] = lblVrtx[0] + 1;
lblVrtx[2] = lblVrtx[0] + (NX+1);
lblVrtx[3] = lblVrtx[2] + 1;
for (j=0; j<4; ++j) {
    for (i=0; i<4; ++i) {
        val = GlbMat[lblVrtx[i]*9+nbr[i][j]];
        GlbMat[lblVrtx[i]*9+nbr[i][j]] = val + eltMat[i][j];
        GlbMatNdx[lblVrtx[i]*9+nbr[i][j]] = lblVrtx[j];
    }
}
}
}

/*
fp = fopen("GlbMat.dat", "w");
for (i=0; i<(NX+1)*(NY+1); ++i) {
    fprintf(fp, "%6d ", i);
    for (j=0; j<9; ++j) fprintf(fp, "%14.6f ", GlbMat[i*9+j]);
    fprintf(fp, "\n");
}
fclose(fp);
*/

return;
}

// ELLAM: tracking characteristics based on the explicit Euler
// 40 micro steps

void ELLAM::trknExEuler(double &xstar, double &ystar,
    double xn, double yn, double tn, double tn1)

```

```

{
  int m;
  double deltat = (tn1-tn)/40;
  double vx, vy, xm, xm1, ym, ym1;

  xm = xn;
  ym = yn;

  for (m=1; m<=40; ++m) {
    velxy(vx, vy, xm, ym, tn);
    xm1 = xm + vx*deltat;
    ym1 = ym + vy*deltat;
    xm = xm1;
    ym = ym1;
  }

  xstar = xm1;
  ystar = ym1;

  return;
}

// ELLAM: assembling the global right-hand side for the old mass
// Un1: numerical solution at time t_{n-1}

void ELLAM::asmGlbRHS40ldMass(double *GlbRHS, double *Un1, double tn)
{
  // FILE *fp;
  int i, j, k, ie, je, kq, istar, jstar;
  int lblVrtx[4];
  double x0, y0, x1, y1, xc, yc, xel, yel;
  double intgr1, xstar, ystar, xx0, xx1, yy0, yy1;
  double U00, U10, U01, U11, vx, vy, w00, w10, w01, w11;
  double xq[9], yq[9], Ustar[9], phiq[2][2][9], eltRHS[4];

  for (je=1; je<=NY; ++je) {
    y0 = Y[je-1]; y1 = Y[je]; yc = 0.5*(y0+y1); yel = y1 - y0;

```

```

for (ie=1; ie<=NX; ++ie) {
  x0 = X[ie-1];  x1 = X[ie];  xc = 0.5*(x0+x1);  xel = x1 - x0;

  // Global indices of the four vertices
  lblVrtx[0] = (je-1)*(NX+1) + (ie-1);
  lblVrtx[1] = lblVrtx[0] + 1;
  lblVrtx[2] = lblVrtx[0] + (NX+1);
  lblVrtx[3] = lblVrtx[2] + 1;

  // Gaussian quadrature points and test function values
  for (kq=0; kq<GQR3npts; ++kq) {
    xq[kq] = xc + (xel/2)*GQR3wab[kq][1];
    yq[kq] = yc + (yel/2)*GQR3wab[kq][2];
    phiq[0][0][kq] = ((x1-xq[kq])/(x1-x0))*((y1-yq[kq])/(y1-y0));
    phiq[1][0][kq] = ((xq[kq]-x0)/(x1-x0))*((y1-yq[kq])/(y1-y0));
    phiq[0][1][kq] = ((x1-xq[kq])/(x1-x0))*((yq[kq]-y0)/(y1-y0));
    phiq[1][1][kq] = ((xq[kq]-x0)/(x1-x0))*((yq[kq]-y0)/(y1-y0));
  }

  // Back-tracking the quadrature points
  for (kq=0; kq<GQR3npts; ++kq) {
    velxy(vx, vy, xq[kq], yq[kq], tn);
    // vx = velx(xq[kq], yq[kq], tn);
    // vy = vely(xq[kq], yq[kq], tn);
    xstar = xq[kq] - vx*Deltat;
    ystar = yq[kq] - vy*Deltat;

    if (xstar<=XA || xstar>=XB || ystar<=YC || ystar>=YD) {
      Ustar[kq] = 0;
      continue;
    }

    istar = (int)floor((xstar-XA)/Deltax);
    jstar = (int)floor((ystar-YC)/Deltay);
    xx0 = X[istar];  xx1 = X[istar+1];
    yy0 = Y[jstar];  yy1 = Y[jstar+1];
  }
}

```

```

    U00 = Un1[jstar*(NX+1)+istar];
    U10 = Un1[jstar*(NX+1)+istar+1];
    U01 = Un1[(jstar+1)*(NX+1)+istar];
    U11 = Un1[(jstar+1)*(NX+1)+istar+1];
    w00 = ((xx1-xstar)/(xx1-xx0))*((yy1-ystar)/(yy1-yy0));
    w10 = ((xstar-xx0)/(xx1-xx0))*((yy1-ystar)/(yy1-yy0));
    w01 = ((xx1-xstar)/(xx1-xx0))*((ystar-yy0)/(yy1-yy0));
    w11 = ((xstar-xx0)/(xx1-xx0))*((ystar-yy0)/(yy1-yy0));
    Ustar[kq] = U00*w00 + U10*w10 + U01*w01 + U11*w11;
}

// Old mass
k = 0;
for (j=0; j<2; ++j) {
    for (i=0; i<2; ++i) {
        intgr1 = 0.0;
        for (kq=0; kq<GQR3npts; ++kq)
            intgr1 += Ustar[kq]*phiq[i][j][kq]*GQR3wab[kq][0];
        intgr1 *= xel*yel;
        eltRHS[k] = intgr1;
        k++;
    }
}

// Assembling the element RHS into the global RHS
for (k=0; k<4; ++k) G1bRHS[lblVrtx[k]] += eltRHS[k];
}
}

return;
}

```

// ELLAM: assembling the global right-hand side for the source term

```

void ELLAM::asmG1bRHS4Srs(double *G1bRHS, double tn)
{
    int i, j, k, ie, je, kq;

```

```

int lblVrtx[4];
double intgr1, x0, y0, x1, y1, xc, yc, xel, yel;
double xq[9], yq[9], fq[9], phiq[2][2][9], eltRHS[4];

for (je=1; je<=NY; ++je) {
  y0 = Y[je-1];  y1 = Y[je];  yc = 0.5*(y0+y1);  yel = y1 - y0;
  for (ie=1; ie<=NX; ++ie) {
    x0 = X[ie-1];  x1 = X[ie];  xc = 0.5*(x0+x1);  xel = x1 - x0;

    // Global indices of the four vertices
    lblVrtx[0] = (je-1)*(NX+1) + (ie-1);
    lblVrtx[1] = lblVrtx[0] + 1;
    lblVrtx[2] = lblVrtx[0] + (NX+1);
    lblVrtx[3] = lblVrtx[2] + 1;

    // Gaussian quadrature points and function values
    for (kq=0; kq<GQR3npts; ++kq) {
      xq[kq] = xc + (xel/2)*GQR3wab[kq][1];
      yq[kq] = yc + (yel/2)*GQR3wab[kq][2];
      phiq[0][0][kq] = ((x1-xq[kq])/(x1-x0))*((y1-yq[kq])/(y1-y0));
      phiq[1][0][kq] = ((xq[kq]-x0)/(x1-x0))*((y1-yq[kq])/(y1-y0));
      phiq[0][1][kq] = ((x1-xq[kq])/(x1-x0))*((yq[kq]-y0)/(y1-y0));
      phiq[1][1][kq] = ((xq[kq]-x0)/(x1-x0))*((yq[kq]-y0)/(y1-y0));
      fq[kq] = srs(xq[kq], yq[kq], tn);
    }

    // Element RHS from the source term
    k = 0;
    for (j=0; j<2; ++j) {
      for (i=0; i<2; ++i) {
        intgr1 = 0.0;
        for (kq=0; kq<GQR3npts; ++kq)
          intgr1 += fq[kq]*phiq[i][j][kq]*GQR3wab[kq][0];
        intgr1 *= xel*yel;
        eltRHS[k] = Deltat*intgr1;
        k++;
      }
    }
  }
}

```

```

        // Assembling the element RHS into the global RHS
        for (k=0; k<4; ++k)  GlbRHS[lblVrtx[k]] += eltRHS[k];
    }
}

return;
}

// ELLAM: modify the global system based on
// a homogeneous Dirichlet boundary condition

void ELLAM::modGlbSysDirichletBndryCond(double *GlbMat, double *GlbRHS)
{
    int i, j, k, l;

    // cout << "In modGlbSysDirichletBndryCond...\n";

    j = 0; // Domain bottom side
    for (i=0; i<=NX; ++i) {
        k = j*(NX+1) + i;
        for (l=0; l<9; ++l)  GlbMat[k*9+l] = 0.0;
        GlbMat[k*9+4] = 1.0;
        GlbRHS[k] = 0.0;
    }

    j = NY; // Domain top side
    for (i=0; i<=NX; ++i) {
        k = j*(NX+1) + i;
        for (l=0; l<9; ++l)  GlbMat[k*9+l] = 0.0;
        GlbMat[k*9+4] = 1.0;
        GlbRHS[k] = 0.0;
    }

    i = 0; // Domain left side
    for (j=1; j<=(NY-1); ++j) {
        k = j*(NX+1) + i;

```

```

    for (l=0; l<9; ++l)  GlbMat[k*9+1] = 0.0;
    GlbMat[k*9+4] = 1.0;
    GlbRHS[k] = 0.0;
}

i = NX; // Domain right side
for (j=1; j<=(NY-1); ++j) {
    k = j*(NX+1) + i;
    for (l=0; l<9; ++l)  GlbMat[k*9+1] = 0.0;
    GlbMat[k*9+4] = 1.0;
    GlbRHS[k] = 0.0;
}

return;
}

// ELLAM: solve the nonsymmetric global linear system
// by BiCGStab with the simple diagonal preconditioner
// a specialized version
// cf: p.27 of the SIAM Templates book

int ELLAM::slvGlbSysBiCGStab(int n, double *x,
    double *A, int *M, double *b, double tol)
{
    int i, j, k, kmax;
    double alpha, beta, omega, res, rho1, rho2, dpst, dptt;
    double *B, *p, *phat, *r, *rhat, *s, *shat, *t, *v;

    B = new double[n];
    p = new double[n];
    r = new double[n];
    s = new double[n];
    t = new double[n];
    v = new double[n];
    phat = new double[n];
    rhat = new double[n];
    shat = new double[n];

```

```

kmax = n;

for (i=0; i<n; ++i) B[i] = A[i*9+4];

for (i=0; i<n; ++i) {
    r[i] = b[i];
    for (j=0; j<9; ++j) r[i] -= A[i*9+j]*x[M[i*9+j]];
}

for (i=0; i<n; ++i) rhat[i] = r[i];

res = 0;
for (i=0; i<n; ++i) res += r[i]*r[i];

// tol *= res;

for (k=1; k<=kmax; ++k) {
    rho1 = 0;
    for (i=0; i<n; ++i) rho1 += r[i]*rhat[i];

    if (rho1==0) {return 2;}

    if (k==1) {
        for (i=0; i<n; ++i) p[i] = r[i];
    } else {
        beta = (rho1/rho2)*(alpha/omega);
        for (i=0; i<n; ++i) {
            p[i] -= omega*v[i];
            p[i] = r[i] + beta*p[i];
        }
    }

    for (i=0; i<n; ++i) phat[i] = p[i]/B[i];

    for (i=0; i<n; ++i) {
        v[i] = 0;
        for (j=0; j<9; ++j) v[i] += A[i*9+j]*phat[M[i*9+j]];
    }
}

```

```
}

alpha = 0;
for (i=0; i<n; ++i) alpha += rhat[i]*v[i];
alpha = rho1/alpha;

for (i=0; i<n; ++i) s[i] = r[i] - alpha*v[i];

res = 0;
for (i=0; i<n; ++i) res += v[i]*v[i];

if (res<tol) {
    for (i=0; i<n; ++i) x[i] += alpha*phat[i];
    return 0;
}

for (i=0; i<n; ++i) shat[i] = s[i]/B[i];

for (i=0; i<n; ++i) {
    t[i] = 0;
    for (j=0; j<9; ++j) t[i] += A[i*9+j]*shat[M[i*9+j]];
}

dpst = 0;
dptt = 0;
for (i=0; i<n; ++i) {
    dpst += s[i]*t[i];
    dptt += t[i]*t[i];
}
omega = dpst/dptt;

for (i=0; i<n; ++i) {
    x[i] += alpha*phat[i] + omega*shat[i];
    r[i] = s[i] - omega*t[i];
}

rho2 = rho1;
```

```
    res = 0;
    for (i=0; i<n; ++i) res += r[i]*r[i];

    if (res<tol) {return 0;}
    if (omega==0) {return 3;}
}

delete[] B, p, phat, r, rhat, s, shat, t, v;
return 1;
}

// ELLAM: set an initial condition

void ELLAM::setInitCond(double *U, int nx, int ny, int order)
{
    int i, j, k;

    if (nx!=NX || ny!=NY) {
        cout << "Mesh mismatch!\n";
        exit(-1);
    }

    U0 = new double[(NX+1)*(NY+1)];

    if (order==0) {
        for (j=0; j<=NY; ++j) {
            for (i=0; i<=NX; ++i) {
                k = j*(NX+1) + i;
                U0[k] = U[k];
            }
        }
    }

    return;
}
```

```
// ELLAM: get the final solution

void ELLAM::getFinalSln(double *U, int nx, int ny, int order)
{
    int i, j, k;

    if (nx!=NX || ny!=NY) {
        cout << "Mesh mismatch!\n";
        exit(-1);
    }

    if (order==0) {
        for (j=0; j<=NY; ++j) {
            for (i=0; i<=NX; ++i) {
                k = j*(NX+1) + i;
                U[k] = UT[k];
            }
        }
    }

    return;
}

// ELLAM: execution (time-marching)
// verbosity: 0: none, 1: minimum, 2: medium

void ELLAM::execute(int verbosity)
{
    FILE *fp;
    int i, j, n, szGlbSys;
    double tn, tn1;
    double *GlbMat, *GlbRHS, *sln, *Un, *Un1, *Utmp;
    int *GlbMatNdx;

    szGlbSys = (NX+1)*(NY+1);

    sln = new double[szGlbSys];
```

```

Un = new double[szGlbSys];
Un1 = new double[szGlbSys];
GlbMat = new double[szGlbSys*9];
GlbMatNdx = new int[szGlbSys*9];
GlbRHS = new double[szGlbSys];

asmGlbMat(GlbMat, GlbMatNdx);

Un1 = U0;
if (verbosity>0) cout << "ELLAM time-marching...\n";
for (n=1; n<=NT; ++n) {
    tn = n*Deltat;
    tn1 = (n-1)*Deltat;
    if (verbosity>0) cout << "n=" << n << " ";

    for (i=0; i<szGlbSys; ++i) GlbRHS[i] = 0;
    asmGlbRHS4Srs(GlbRHS, tn);
    asmGlbRHS4OldMass(GlbRHS, Un1, tn);
    modGlbSysDirichletBndryCond(GlbMat, GlbRHS);

    for (i=0; i<szGlbSys; ++i) sln[i] = Un1[i];
    slvGlbSysBiCGStab(szGlbSys, sln, GlbMat, GlbMatNdx, GlbRHS, 1E-30);
    for (i=0; i<szGlbSys; ++i) Un[i] = sln[i];

    // Refreshing: swap pointers!
    Utmp = Un1; Un1 = Un; Un = Utmp;
}
if (verbosity>0) cout << "\n";
UT = Un1;

fp = fopen("GlbMat.dat", "w");
for (i=0; i<(NX+1)*(NY+1); ++i) {
    fprintf(fp, "%6d ", i);
    for (j=0; j<9; ++j) fprintf(fp, "%14.6f ", GlbMat[i*9+j]);
    fprintf(fp, "\n");
}
fclose(fp);

```

```

fp = fopen("GlbRHS.dat", "w");
for (i=0; i<(NX+1)*(NY+1); ++i)
    fprintf(fp, "%6d %14.6f\n", i, GlbRHS[i]);
fclose(fp);

delete[] GlbMat, GlbMatNdx, GlbRHS, sln, Un, Un1;
return;
}

```

### 4.3 Mini ELLAM: Examples

The C++ code below has two examples (worked in the previous Chapter).

```

// TstMiniELLAM.cpp
// A small test program for MiniELLAM
// Jiangguo (James) Liu, ColoState, 12/2008 - 03/2009

#include <cmath>
#include <iostream>
#include <stdio.h>
#include <stdlib.h>
#include "MiniELLAM.h"
using namespace std;

double ex0sln(double x, double y, double t)
{
    double a = 1; double b = 1;
    double xc = -0.5; double yc = -0.5;
    double sigma122 = 50;
    double xt = x - xc - a*t;
    double yt = y - yc - b*t;
    double u = exp(-(xt*xt+yt*yt)*sigma122);
    return u;
}

```

```

double ex0velx(double x, double y, double t)
{
    double a = 1.0; return a;
}

double ex0vely(double x, double y, double t)
{
    double b = 1.0; return b;
}

double ex0srs(double x, double y, double t)
{
    double D = 1E-3;
    double a = 1; double b = 1;
    double xc = -0.5; double yc = -0.5;
    double sigma212 = 200; double sigma14 = 10000;
    double xt = x - xc - a*t;
    double yt = y - yc - b*t;
    double u = ex0sln(x, y, t);
    double f = D*(sigma212-sigma14*(xt*xt+yt*yt))*u;
    return f;
}

double ex1sln(double x, double y, double t)
{
    double sigma22 = 4E-3; double D = 1E-4;
    double xc = -0.5; double yc = 0.0;
    double xstar = cos(4*t)*x + sin(4*t)*y;
    double ystar = -sin(4*t)*x + cos(4*t)*y;
    double xt = xstar - xc;
    double yt = ystar - yc;
    double u = exp(-(xt*xt+yt*yt)/(sigma22+4*D*t));
    u = sigma22/(sigma22+4*D*t)*u;
    return u;
}

double ex1velx(double x, double y, double t) {return -4*y;}

```

```

double ex1vely(double x, double y, double t) {return 4*x;}

double ex1srs(double x, double y, double t) {return 0.0;}

void main()
{
    FILE *fp;
    int i, j, nt, nx, ny;
    double a, b, c, d, hx, hy, t0, tf;
    double *x, *y, *U;
    double *Ex1Vx, *Ex1Vy;
    double PI = 3.141592653589793;

    cout << "OK beginning!\n";

    a = -1;  b = 1;  c = -1;  d = 1;  nx = 128;  ny = 128;
    t0 = 0;  tf = PI/2;  nt = 50;

    hx = (b-a)/nx;
    x = new double[nx+1];
    x[0] = a;
    for (i=1; i<nx; ++i)  x[i] = x[i-1] + hx;
    x[nx] = b;

    hy = (d-c)/ny;
    y = new double[ny+1];
    y[0] = c;
    for (j=1; j<ny; ++j)  y[j] = y[j-1] + hy;
    y[ny] = d;

    Ex1Vx = new double[(nx+1)*(ny+1)];
    Ex1Vy = new double[(nx+1)*(ny+1)];
    for (j=0; j<=ny; ++j) {
        for (i=0; i<=nx; ++i) {
            Ex1Vx[j*(nx+1)+i] = ex1velx(x[i], y[j], t0);
            Ex1Vy[j*(nx+1)+i] = ex1vely(x[i], y[j], t0);
        }
    }
}

```

```

    }
}

U = new double[(nx+1)*(ny+1)];
for (j=0; j<=ny; ++j)
    for (i=0; i<=nx; ++i)
        U[j*(nx+1)+i] = ex1sln(x[i], y[j], t0);

fp = fopen("U0.dat", "w");
for (j=0; j<=ny; ++j)
    for (i=0; i<=nx; ++i)
        fprintf(fp, "%12.6f %12.6f %12.6f\n", x[i], y[j], U[j*(nx+1)+i]);
fclose(fp);

ELLAM ellam;
ellam.setMesh(a, b, c, d, nx, ny);
ellam.setTime(t0, tf, nt);
// ellam.setVelFxn(ex1velx, ex1vely);
ellam.setVelData(Ex1Vx, Ex1Vy, nx, ny, 0);
ellam.setDiffConst(1E-4);
ellam.setSrsFxn(ex1srs);
ellam.setInitCond(U, nx, ny, 0);
ellam.execute(1);
ellam.getFinalSln(U, nx, ny, 0);

fp = fopen("UT.dat", "w");
fprintf(fp, "%5d %5d\n", nx, ny);
for (j=0; j<=ny; ++j)
    for (i=0; i<=nx; ++i)
        fprintf(fp, "%12.6f %12.6f %12.6f\n", x[i], y[j], U[j*(nx+1)+i]);
fclose(fp);

delete[] Ex1Vx, Ex1Vy;
delete[] U, x, y;
cout << "Happy ending!\n";
return;
}

```

```
% PlotUT.m
% Plotting 3-dim graph for numerical solution UT
% Jiangguo (James) Liu, ColoState, 02/2009

clc;
clear all;
close all;

fp = fopen('UT.dat', 'r');

v = zeros(2,1);
v = fscanf(fp, '%d', 2);

NX = v(1);
NY = v(2);

X = zeros(NX+1,1);
Y = zeros(NY+1,1);
UT = zeros(NX+1, NY+1);

v = zeros(3,1);

for j = 0 : NY
    for i = 0 : NX
        v = fscanf(fp, '%f', 3);
        X(i+1) = v(1);
        Y(j+1) = v(2);
        UT(i+1,j+1) = v(3);
    end
end

fclose(fp);

figure(1);
mesh(X, Y, UT);
% title('Approx Solution UT');
% zlim([-0.1, 1.1]);
```

```
print -f1 UT.ps
```

```
disp('pause...');  
pause;  
close all;
```

# Appendix A

## List of Abbreviations

The following list might be helpful for understanding my code or other documents.

**abs** absolute / absolute value

**aprx** approximate / approximation

**asm** assemble

**avg** average

**bd** bound

**bdd** bounded

**bdry** boundary

**bk** back / backward

**bkp** backup

**Cart** Cartesian

<b>chara</b>	characteristic(s)
<b>cmplt</b>	complete
<b>cntr</b>	center
<b>comput</b>	compute
<b>cond</b>	condition
<b>const</b>	constant
<b>crd</b>	coordinate
<b>def</b>	definition
<b>deriv</b>	derivative
<b>diam</b>	diameter
<b>diff</b>	differentiation / diffusion
<b>dist</b>	distance
<b>dom</b>	domain
<b>elt</b>	element
<b>eqn</b>	equation
<b>err</b>	error
<b>fwd</b>	forward
<b>fxn</b>	function
<b>fxnl</b>	functional

**gen** general / generate

**geom** geometry

**glb** global

**grp** group

**idx** index (see also **ind,ndx**)

**ind** index (see also **idx,ndx**)

**init** initialization

**int** integer

**integ** integral / integrand / integration

**intvl** interval

**IO** inout / outpout

**itr** iteration

**lbl** label

**lcl** local

**lin** linear

**loc** locate / location

**lvl** level

**mat** matrix

**max** maximal / maximum

<b>mdl</b>	middle
<b>min</b>	minimal / minimum
<b>nbr</b>	neighbor
<b>nd</b>	node
<b>ndx</b>	index (see also <b>ind</b> , <b>idx</b> )
<b>nlin</b>	nonlinear
<b>num</b>	number / numerical
<b>pt</b>	point
<b>ptr</b>	pointer
<b>quad</b>	quadrature
<b>rect</b>	rectangle / rectangular
<b>ref</b>	reference
<b>rhs,RHS</b>	right-hand side
<b>seg</b>	segment(s)
<b>sln</b>	solution
<b>slv</b>	solve
<b>sqr</b>	square
<b>sqrt</b>	square root
<b>srs</b>	source

**stf** stiffness

**sub** sub-

**sys** system

**tol** tolerance

**trl** trial

**trk** tracking

**tst** test

**tyme** time (to avoid conflicts with “time”, which might be reserved in some languages)

**val** value

**vec** vector

**vel** velocity

**vrtx** vertex / vortex

**whl** whole

**wt** weight



# Bibliography

- [1] M.A. Celia, T.F. Russell, I. Herrera, and R.E. Ewing, *An Eulerian-Lagrangian localized adjoint method for the advection-diffusion equation*, Adv. Water Resour., **13** (1990), 187-206.
- [2] G.H. Golub and C.F. Van Loan, *Matrix Computations*, The Johns Hopkins University Press, 3rd ed., 1996.
- [3] J. Liu, *Efficient numerical techniques for advection dominated transport equations*, Ph.D. Thesis, University of South Carolina, 2001.
- [4] J. Liu, B. Popov, H. Wang, and R.E. Ewing, *Convergence analysis of wavelet schemes for convection-reaction equations under minimal regularity assumptions*, SIAM J. Numer. Anal., *To appear*.
- [5] W. Schroeder, K. Martin, and B. Lorensen, *The visualization toolkit: An object-oriented approach to 3D graphics*, 3rd ed., Kitware, 2002.
- [6] H. Wang, H.K. Dahle, R.E. Ewing, M.S. Espedal, R.C. Sharpley, and S. Man, *An ELLAM scheme for advection-diffusion equations in two dimensions*, SIAM J. Sci. Comput., **20** (1999), 2160-2194.